Modeling of Ethylene Polymerization with Difunctional Initiators in Tubular Reactors

P. K. F. Khazraei, R. Dhib

Department of Chemical Engineering, Ryerson University, 350 Victoria Street, Toronto, Ontario M5B 2K3, Canada

Received 11 July 2007; accepted 7 November 2007
DOI 10.1002/app.28429
Published online 10 June 2008 in Wiley InterScience (www.interscience.wiley.com).

ABSTRACT: The severe thermodynamic conditions of the high-pressure ethylene polymerization process hinder ethylene from going to full conversion. One remedy to improve the monomer conversion is to make effective use of difunctional peroxides. Multifunctional peroxides can accelerate the polymerization rate, produce branching, and modify the rheological properties of molten polymers. This article proposes a kinetic model based on a postulated reaction mechanism for ethylene polymerization initiated by difunctional initiators in a high-pressure tubular reactor. Three peroxides suitable for ethylene polymerization were compared for their effectiveness. Compared to dioctanoyl peroxide, the two difunctional peroxides considered performed much better for the higher temperature regions of the reactor and gave ethylene conversions nearly twice as high for only half of the initial amount of dioctanoyl. They also generated low-density polyethylene polymer with a broader molecular weight distribution and longer chain branching. These two important polymer characteristics can influence the end-product rheological properties. Injecting fresh ethylene at different points along the reactor improved the conversion and produced more branched polymer. © 2008 Wiley Periodicals, Inc. J Appl Polym Sci 109: 3908–3922, 2008

Key words: branched; modeling; polyethylene (PE)

INTRODUCTION

Polymerization conditions, including the reaction thermodynamic conditions, chemical initiator, mixture flow, and reactor type, are predominantly responsible for shaping the properties of a polymeric end product. Polymers differ in their properties and are accordingly selected for a particular commercial application. Despite the recent evident success of producing polyolefins in relatively low-pressure gas phase and solutions processes, high-pressure olefin polymerization remains substantially important and competitive. Being an important polymer commonly used in the manufacture of a wide range of engineering and commodity plastics, low-density polyethylene (LDPE) is conventionally produced in autoclave and tubular processes at high pressure (P = 1000–3500 atm) and temperature (T = 150–300°C) in the presence of a selected chemical initiator. However, the severe thermodynamic conditions of the polymerization prevent ethylene from going to full conversion, but the reaction system still produces a polymer with interesting and useful characteristics. With regard to the valuable industrial importance of LDPE, improving the process performance is still a major concern in academia and industry. Over the last few decades, a number of academicians and industrialists have incessantly attempted to establish a unified tangible understanding of ethylene polymerization in high-pressure autoclave reactors for both autoclave and tubular reactors.[1–4] However, the setback of obtaining only a limited low conversion of ethylene in high-pressure polymerization has not been resolved and has persistently been an unpleasant discouraging reality despite worthy attempts to improve the conversion upon recycling of the product and apply optimization schemes.[5,6]

A third route to overcoming the problem of limited ethylene conversion inherent in this polymerization process is to examine the effectiveness of multifunctional initiators or difunctional peroxides, in particular. Under thermal effects, organic peroxides exhibit different rates of decomposition because of their dissimilar half-life temperatures. In the quest to make new efficient initiators to enhance polymer production, a profound comprehension of the kinetic mechanism of initiator fragmentation was the core of several studies.[7–9] The proper use of a peroxide as an initiator for a given polymerization depends strongly on its half-life temperature and reactivity. Nevertheless, initiator efficiency is still a controversial issue. For relatively low-temperature polymerization processes, such as those for styrene and methyl methacrylates, it has been experimentally determined that a multifunctional peroxide not only

Correspondence to: R. Dhib (rdhib@ryerson.ca).
Contract grant sponsor: Natural Sciences and Engineering Research Council (NSERC)-Canada.
Contract grant sponsor: Ryerson University.

boosts polymerization rate but can also introduce branching in some cases.[9] Recently, Scorah et al.[10] conducted experimental and theoretical studies on the polymerization of styrene and methyl methacrylate and proved that branched polymers can be produced when a tetrafunctional peroxide is used. Multifunctional initiators can also crosslink with molten polymers and modify its properties. Perez et al.[11] conducted an interesting experimental study and revealed the impact of a difunctional peroxide on the magnitude of the viscous and elastic modulus of high-density polyethylene. Recently, Kondratiev and Ivantchev[12] experimentally tested new organic peroxides suitable for high-pressure polymerization conditions and thoroughly discussed the drawbacks of the use of oxygen alone as an initiator.

Focusing on the chemistry and kinetics of organic peroxides convenient for the polymerization of ethylene in high-pressure reactors, Luft and coworkers[13,14] carried out a series of sound studies on the peroxide kinetic decomposition, reaction rates, effectiveness, and impact on polyethylene (PE) end products. A number of initiators were experimentally tested for the production of LDPE polymers. The ethylene conversion rate, peroxide consumption, and product properties were analyzed through experimental observations. The consumed amount of each initiator constituted the basic criterion for assessing the initiator effectiveness. A simplified kinetic model was developed for the reaction mechanism, but it did not account for the dual functionality of some of the initiators. With the exception of the few aforementioned experimental studies on high-pressure ethylene polymerizations and the theoretical approach of Dhib and Al-Nidawy,[15] work in the literature on multifunctional initiators is very limited, despite their kinetic potential to promote LDPE production and impact the molecular and structural features of a polymer. Obviously, there is a need to thoroughly understand the physicochemical behavior of olefin polymerization with this type of initiator under elevated pressure and temperature conditions.

This study proposes a kinetic model based on a postulated reaction mechanism, which accommodates the use of difunctional peroxides for polymerizing ethylene in high-pressure tubular reactors. The effect of multiple injection points and the production of branching are discussed as well.

REACTION MECHANISM WITH DIFUNCTIONAL INITIATORS

Thermal decomposition of difunctional initiation

A broad spectrum of initiators is available to make polymers of various grades to meet diverse end-use requirements. By properly selecting an effective initiator, one can simultaneously achieve a high monomer conversion and polymer molecular weight. The presence of two or more oxygen–oxygen bonds in multifunctional peroxides makes their kinetic decomposition into radical fragments quite particular. Two investigations[13,16] with independent approaches concluded that the eventual formation of diradicals is unlikely to occur. In particular, for symmetrical peroxides in a high-pressure process, Luft and Seidl[13] investigated a few schemes of peroxide decomposition into radical fragments to produce hydrocarbons. Therefore, upon heating, a difunctional initiator is likely to fragment into two radical species as

$$\mathrm{R_1{-}OO{-}R_2{-}OO{-}R_1} \xrightarrow{2K_{d1}} \mathrm{R_1{-}O^\bullet} + \mathrm{R_1{-}OO{-}R_2{-}O^\bullet} \quad (1)$$

Or symbolically

$$\mathrm{I} \xrightarrow{2K_{d1}} \mathrm{R}^\bullet_{in} + \tilde{\mathrm{R}}^\bullet_{in} \quad (2)$$

where R_1 and R_2 are the organic groups of the peroxide and K_{d1} is the decomposition rate constant of the original difunctional peroxide. Both initiator fragments, the primary initiator radical fragment ($R^\bullet_{in}$) and the initiator radical fragment with one undecomposed peroxide ($\tilde{R}^\bullet_{in}$), participate in the polymerization process and are capable of generating independent polymer chains. The polymer chain associated with the undecomposed peroxide radical $\tilde{R}^\bullet_{in}$ behaves as a macro peroxide radical, and subsequently, it becomes a part of the initiation step. As a result, the thermal stability of the peroxide bridge is altered when the neighboring organic groups break away.

Reaction mechanism

A detailed kinetic mechanism of ethylene polymerization with difunctional peroxides in a high-pressure autoclave reactor was proposed previously.[15] It gives rise to a series of chain reactions based on few assumptions: no diradical formation and negligible chain transfer to telogens (propylene). M, I, and P are the monomer (ethylene) molecule, the difunctional initiator molecule, and the polymer (PE) molecule, respectively.

Chemical initiation by difunctional peroxide

$$\mathrm{I} \xrightarrow{2K_{d1}} \mathrm{R}^\bullet_{in} + \tilde{\mathrm{R}}^\bullet_{in}$$

$$\mathrm{R}^\bullet_{in} + \mathrm{M} \xrightarrow{K_1} \mathrm{R}^\bullet_1$$

$$\tilde{\mathrm{R}}^\bullet_{in} + \mathrm{M} \xrightarrow{K_2} \tilde{\mathrm{R}}^\bullet_1$$

$$\tilde{\mathrm{P}}_r \xrightarrow{K_{d2}} \mathrm{R}^\bullet_{in} + \mathrm{R}^\bullet_r \quad r \geq 2$$

$$\tilde{\tilde{\mathrm{P}}}_r \xrightarrow{2K_{d2}} \mathrm{R}^\bullet_{in} + \tilde{\mathrm{R}}^\bullet_r \quad r \geq 2$$

where K_1 and K_2 are the rate constants for initiation, $\tilde{P}_r$ is the dead polymer concentration with one undecomposed peroxide, $R_r^\bullet$ is a radical of chain length r, $\tilde{\tilde{P}}_r$ is the dead polymer concentration with two undecomposed peroxides, K_{d2} is the decomposition rate constant of peroxide with one undecomposed radical, and $\tilde{R}_r^\bullet$ is a macroradical fragment of chain length r with one undecomposed peroxide.

Thermal initiation

$$3M \xrightarrow{K_{th}} 2R_1^\bullet$$

where K_{th} is rate constant for thermal initiation.

Propagation

$$R_r^\bullet + M \xrightarrow{K_p} R_{r+1}^\bullet \quad r \geq 1$$

$$\tilde{R}_r^\bullet + M \xrightarrow{K_p} \tilde{R}_{r+1}^\bullet \quad r \geq 1$$

where K_p is the rate constant for propagation.

Termination

$$R_r^\bullet + R_s^\bullet \xrightarrow{K_{tc}} P_{r+s} \quad r, s \geq 1$$

$$R_r^\bullet + \tilde{R}_s^\bullet \xrightarrow{K_{tc}} \tilde{P}_{r+s} \quad r, s \geq 1$$

$$\tilde{R}_r^\bullet + \tilde{R}_s^\bullet \xrightarrow{K_{tc}} \tilde{\tilde{P}}_{r+s} \quad r, s \geq 1$$

where $R_s^\bullet$ is a radical of chain length s, K_{tc} is the rate constant for termination, and $\tilde{R}_s^\bullet$ is a macroradical fragment of chain length s with one undecomposed peroxide.

Transfer to monomer

$$R_r^\bullet + M \xrightarrow{K_{tfm}} P_r + R_1^\bullet \quad r \geq 1$$

$$\tilde{R}_r^\bullet + M \xrightarrow{K_{tfm}} \tilde{P}_r + R_1^\bullet \quad r \geq 1$$

where K_{tfm} is the rate constant for transfer to monomer and P_r is the dead polymer molecule.

β scission to secondary radicals

$$R_{r+1}^\bullet \xrightarrow{K_\beta} P_r + R_1^\bullet \quad r \geq 1$$

$$\tilde{R}_{r+1}^\bullet \xrightarrow{K_\beta} \tilde{P}_r + R_1^\bullet \quad r \geq 1$$

where K_β is the rate constant for β scission.

Intermolecular transfer (back-biting)

$$R_r^\bullet \xrightarrow{K_b} R_{br}^\bullet \quad r \geq 1$$

$$\tilde{R}_r^\bullet \xrightarrow{K_b} \tilde{R}_{br}^\bullet \quad r \geq 1$$

where K_b is the rate constant for back-biting. $R_{br}^\bullet$ is the polymer molecule produced in the backbiting reaction.

Transfer to polymer

$$R_r^\bullet + P_s \xrightarrow{K_{fp}} P_r + R_s^\bullet \quad r, s \geq 1$$

$$R_r^\bullet + \tilde{P}_s \xrightarrow{K_{fp}} \tilde{P}_r + R_s^\bullet \quad r, s \geq 1$$

$$\tilde{R}_r^\bullet + P_s \xrightarrow{K_{fp}} P_r + \tilde{R}_s^\bullet \quad r, s \geq 1$$

$$\tilde{R}_r^\bullet + \tilde{P}_s \xrightarrow{K_{fp}} \tilde{P}_r + \tilde{R}_s^\bullet \quad r, s \geq 1$$

where $R_r^\bullet$ ($r \geq 1$) is the regular radical, K_{fp} is the rate constant for transfer to polymer, $\tilde{R}_r^\bullet$ ($r \geq 1$) is the macroradical with one undecomposed peroxide, P_r (R—R) is the dead polymer molecule, and $\tilde{P}_r$ (R—$\tilde{R}$) is the dead polymer molecule with one undecomposed peroxide. The factor 2 multiplying K_{d1} and K_{d2} stands for the dual functionality of peroxides in the initiator and $\tilde{\tilde{P}}_r$.

MODEL OF HIGH-PRESSURE TUBULAR REACTOR

Live radical molar concentrations

Writing a molar balance for primary radicals $R_{in}^\bullet$ and $\tilde{R}_{in}^\bullet$ and applying the steady-state hypothesis for short-lived initiator primary radicals resulted in the initiation rates shown next.

For a monofunctional initiator (dioctanoyl peroxide)

$$R_I = 2K_{th}[M]^3 + 2f_1K_{d1}[I] \tag{3}$$

where R_I is the rate of initiation without undecomposed peroxide, [M] is the monomer concentration, f_1 is the efficiency of the original initiator, and [I] is the initiator concentration. For a difunctional peroxide such as perketals, two different rates emerging from $R_{in}^\bullet$ and $\tilde{R}_{in}^\bullet$ are defined, respectively, as

$$R_I = 2K_{th}[M]^3 + 2f_1K_{d1}[I] + f_2K_{d2}(\tilde{\mu}_0 + 2\tilde{\tilde{\mu}}_0) \tag{4}$$

$$\tilde{R}_I = 2f_1K_{d1}[I] \tag{5}$$

where f_2 is the efficiency of the initiator with undecomposed peroxide, $\tilde{\mu}_i$ is the moment of the dead polymer molecule with one undecomposed peroxide ($\tilde{P}$), $\tilde{\tilde{\mu}}_i$ is the moment of the dead polymer molecule with two undecomposed peroxides ($\tilde{\tilde{P}}$), and $\tilde{R}_I$ is the rate of initiation with undecomposed peroxide. The initiator efficiencies f_1 and f_2 account for the fraction of initiator amount that actually participates in the polymerization of ethylene. The method of moments defined in the Appendix is a straightforward and compact way to determine the concentrations of live and dead polymer chains. Thus, performing molar balances on the growing temporary polymer radicals $R_r^\bullet$ and $\tilde{R}_r^\bullet$ and assuming a quasi-steady-state hypothesis leads to the algebraic expressions for the live radical moments, λ_i and $\tilde{\lambda}_i$, where λ_i is the moment of the live temporary polymer radical and $\tilde{\lambda}_i$ is the moment of the live temporary polymer radical with one undecomposed peroxide:

$$\tilde{\lambda}_0 = \frac{\tilde{R}_I + 2f_2K_{d2}\tilde{\tilde{\mu}}_0}{K_{tfm}[\mathrm{M}] + K_\beta + K_{tc}\lambda_{to}} \tag{6}$$

$$\lambda_0 = \frac{R_I + \left(K_{tfm}[\mathrm{M}] + K_\beta\right)\tilde{\lambda}_0 + f_2K_{d2}\tilde{\mu}_0}{K_{tc}\lambda_{to}} \tag{7}$$

where λ_{to} is the total concentration of radicals. Combining eqs. (6) and (7) gives an analytical expression for λ_{to}:

$$\lambda_{to} = \sqrt{\frac{R_I + \tilde{R}_I + f_2K_{d2}\left(\tilde{\mu}_0 + 2\tilde{\tilde{\mu}}_0\right)}{K_{tc}}} \tag{8}$$

The rate of polymerization (R_p) is given by

$$R_p = K_p[M]\lambda_{to} \tag{9}$$

where $[M]$ is the monomer concentration. The first and second moments are computed from

$$\lambda_1 = \frac{R_I + (K_{tfm}[\mathrm{M}] + K_\beta)\lambda_{to} + f_2K_{d2}\tilde{\mu}_1}{K_{tc}\lambda_{to} + K_{tfm}[\mathrm{M}] + K_\beta + K_{fp}(\mu_1 + \tilde{\mu}_1)} + \frac{K_p[\mathrm{M}]\lambda_0 + K_{fp}(\mu_2 + \tilde{\mu}_2)\lambda_0}{K_{tc}\lambda_{to} + K_{tfm}[\mathrm{M}] + K_\beta + K_{fp}(\mu_1 + \tilde{\mu}_1)} \tag{10}$$

$$\tilde{\lambda}_1 = \frac{\tilde{R}_I + 2f_2K_{d2}\tilde{\tilde{\mu}}_1 + K_p[\mathrm{M}]\tilde{\lambda}_0 + K_{fp}(\mu_2 + \tilde{\mu}_2)\tilde{\lambda}_0}{K_{tc}\lambda_{to} + K_{tfm}[\mathrm{M}] + K_\beta + K_{fp}(\mu_1 + \tilde{\mu}_1)} \tag{11}$$

$$\lambda_2 = \frac{R_I + f_2K_{d2}\tilde{\mu}_2 + K_p[\mathrm{M}](2\lambda_1 + \lambda_0) + (K_{tfm}[\mathrm{M}] + K_\beta)\lambda_{to} + K_{fp}(\mu_3 + \tilde{\mu}_3)\lambda_0}{K_{tc}\lambda_{to} + K_{tfm}[\mathrm{M}] + K_\beta + K_{fp}(\mu_1 + \tilde{\mu}_1)} \tag{12}$$

$$\tilde{\lambda}_2 = \frac{\tilde{R}_I + 2f_2K_{d2}\tilde{\tilde{\mu}}_2 + K_p[\mathrm{M}]\left(2\tilde{\lambda}_1 + \tilde{\lambda}_0\right) + K_{fp}(\mu_3 + \tilde{\mu}_3)\tilde{\lambda}_0}{K_{tc}\lambda_{to} + K_{tfm}[\mathrm{M}] + K_\beta + K_{fp}(\mu_1 + \tilde{\mu}_1)} \tag{13}$$

where μ_i is the moment of the polymer molecule. Because of the complex nature of the high-pressure PE process, a wide variation of kinetic parameter estimates is reported in the literature.[6]

Under normal experimental conditions, the values of K_p and K_{tc} cannot be obtained independently. Most investigators agree on calculating the value of the combined parameter $K_p/K_{tc}^{0.5}$; however values of K_p and K_{tc} reported in the literature show large variations. Therefore, one of the two parameters must be estimated independently. For instance, Goto et al.[1] gave an interesting approach. The values of the reaction rate constants of ethylene polymerization and the three initiators considered are provided in Tables I and II, respectively. Most of the rate constants were taken from a previous study.[15]

Tubular reactor model

An industrial LDPE high-pressure tubular reactor is a spiral-wrapped metallic pipe with a length up to 1500 m and a diameter of about 60 mm, and it oper-

TABLE I
Reaction Rate Constants of Ethylene Polymerization

Rate constant	$k = A\exp(-E/R_1T - \Delta vP/R_2T)$		
	A (1/s)	E (Cal/mol)	Δv (cm^3/mol)
K_{th}	6.04×10^3	38,660.61	0.00
K_p	5.12×10^5	4,210.00	−5.6
K_{tc}	2.53×10^9	3,374.94	9.2
K_{tfm}	1.20×10^4	14,400.00	20
K_{fp}	1.8×10^5	9,400.00	0.00
K_b	3.27×10^5	7,474.13	0.00
K_β	1.4×10^9	19,300.00	9.99

k = thermal conductivity of the reaction mixture; A = frequency factor; E = activation energy; Δv = activation volume. R_1 = 1.98 cal mol^{-1} K^{-1}; R_2 = 82 cm^3 atm mol^{-1} K^{-1}.

TABLE II
Decomposition Rate Constants of the Peroxide Initiators

	Rate		
	$k_{d1} = A_1 \exp(-E_1/R_1T - \Delta v_1 P/R_2T)$ $k_{d2} = A_2 \exp(-E_2/R_1T - \Delta v_2 P/R_2T)$		
Initiator	A_1/A_2 (1/s)	E_1/E_2 (cal/mol)	$\Delta v_1/\Delta v_2$ (cm^3/mol)
DCT	$1.834 \times 10^{14}/0.00$	30,631.70 0.00	5.9/0.00
BU	$7.875 \times 10^{15}/6.04 \times 10^{13}$	42,731.13 41,943.11	28/11.15
DHBPPI	$1.812 \times 10^{16}/6.04 \times 10^{17}$	43,037.28 43,766.72	25/22.3

The subscripts 1 and 2 refer to the original difunctional peroxide and the secondary peroxide with undecomposed radical, respectively.

ates at a temperature and pressure up to 300°C and 2800 atm, respectively. In the reactor arrangement, as shown in Figure 1, a three zone tubular reactor with a length of 1000 m and a diameter of 60 mm is considered.

The preheating zone length covers 30% of the total reactor length, whereas the reaction zone covers 37% and the cooling zone covers 33%. The feed stream consists of ethylene and a peroxide initiator. Steam is used in the first portion of the reactor to heat the feed to the required reaction temperature. Cold water is used in subsequent portions to drive out the excess heat of polymerization. Thus, a nonisothermal reactor operation is expected, even though heat removal in a tube reactor is much easier than in an autoclave reactor. Obviously, temperature control is primordial to ensure a safe operation of the process, as depolymerization reactions may eventually occur at temperatures exceeding 300°C. An evident advantage of tubular reactor is to inject new initiator and monomer streams along the reactor length. Depending on the number of side-feed injection points, the reactor can be divided accordingly into sections. In this study, a monomer–initiator mixture of 10 kg/s enters the reactor at 120°C and 2400 bar.

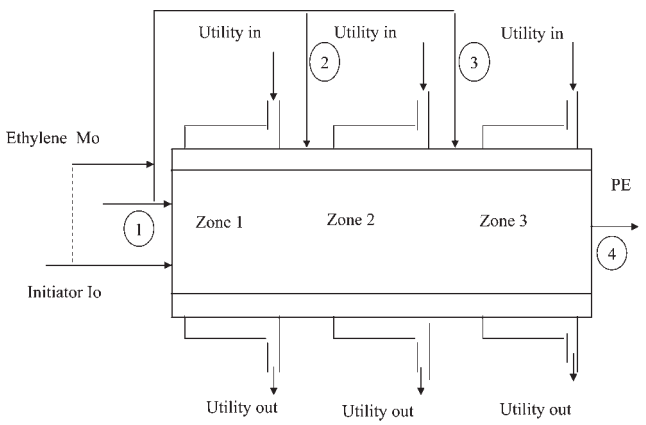

Figure 1 LDPE tubular reactor with injection points for the initiator and monomer.

Next, a kinetic tubular reactor model is developed for ethylene free-radical polymerization initiated by a difunctional peroxide. The reactor model arising from the molar balances of the initiator and monomer, continuity equation, and energy balance is provided next.

Conversion of reactants

$$\frac{d(u[\mathrm{I}])}{dz} = -2K_{d1}[\mathrm{I}] \tag{14}$$

$$\frac{d(u[\mathrm{M}])}{dz} = -R_p[\mathrm{M}] \tag{15}$$

where u is the reaction mixture velocity and z is the reactor length.The component molar flow rate (F_j) is expressed as

$$F_j = \left(\pi D_i^2/4\right) uC_j \tag{16}$$

where j stands for the monomer or initiator, D_i is the inside diameter of the reactor, and C_j is the molar concentration. Thus, the molar flow depends on both the molar concentrations and the reacting mixture velocity along the reactor length.

Continuity equation

$$\frac{\partial(\rho u)}{\partial z} = 0 \tag{17}$$

where ρ is the density.

Energy balance

$$\frac{dT}{dz} = \frac{(-\Delta H_R)LR_p}{\rho\, u\, C_p} + \frac{UA_p(T - T_c)}{\rho\, u\, A_s\, C_p} \tag{18}$$

where $-\Delta H_R$ is the heat of reaction, L is the reactor length, U is the overall heat-transfer coefficient, A_p is

the pipe surface area, T_c is the cooling process temperature, and C_p is the heat capacity.

Energy balance for cooling fluid in the reactor jacket

$$\frac{dT_c}{dz} = \pi D_o L U \frac{(T_c - T)}{\dot{m}_c C_{pc}} \tag{19}$$

where D_o is the outer diameter of the reactor and $\dot{m}_c$ is the cooling mass flow rate.

Pressure drop

The reactor pressure affects the rates of reaction and the thermodynamic properties of the reacting mixture. The pressure drops along the reactor length, and it is assumed that the flow is a turbulent regime. Therefore, a momentum balance gives rise to the following pressure drop variation:

$$\frac{dP}{dz} = -L\left(2f_r \rho \frac{u^2}{D_i} + \rho\, u \frac{du}{dz}\right) \tag{20}$$

where f_r is the fanning friction factor expressed by

$$f_r^{-0.50} = 4\, \log(f_r^{0.50} Re) - 0.4 \tag{21}$$

where Re is Reynolds number. The numerical solution of eq. (21) to obtain f_r requires an initial guess within the range $0.0791\ Re^{-1/4} < f_r < 0.01$, which according to Zabinsky et al.,[17] is the typical range of values for the friction factor under LDPE reactor conditions.

Polymer model

Considering the moments of each polymer chain defined in the Appendix and writing molar balances for each polymeric species (P, $\tilde{P}$, and $\tilde{\tilde{P}}$) concentration, we developed a polymer model, and it is written as follows.

Dead polymer

$$\frac{d(\mu_0 u)}{dz} = K_{tc}\lambda_0^2/2 + (K_{tfm}[M] + K_\beta)\lambda_0 \tag{22}$$

$$\frac{d(\mu_1 u)}{dz} = K_{tc}\lambda_0\lambda_1 + (K_{tfm}[M] + K_\beta)\lambda_1 + K_{fp}\left((\lambda_1 + \tilde{\lambda}_1)\mu_1 - \lambda_{to}\mu_2\right) \tag{23}$$

$$\frac{d(\mu_2 u)}{dz} = K_{tc}(\lambda_0\lambda_2 + \lambda_1^2) + (K_{tfm}[M] + K_\beta)\lambda_2 + K_{fp}\left((\lambda_2 + \tilde{\lambda}_2)\mu_1 - \lambda_{to}\mu_3\right) \tag{24}$$

Temporary polymer $\tilde{P}$

$$\frac{d(\tilde{\mu}_0 u)}{dz} = K_{tc}\lambda_0\tilde{\lambda}_0 - K_{d2}\tilde{\mu}_0 + (K_{tfm}[M] + K_\beta)\tilde{\lambda}_0 \tag{25}$$

$$\frac{d(\tilde{\mu}_1 u)}{dz} = K_{tc}\left(\lambda_0\tilde{\lambda}_1 + \lambda_1\tilde{\lambda}_0\right) - K_{d2}\tilde{\mu}_1 + (K_{tfm}[M] + K_\beta)\tilde{\lambda}_1 + K_{fp}\left((\lambda_1 + \tilde{\lambda}_1)\tilde{\mu}_1 - \lambda_{to}\tilde{\mu}_2\right) \tag{26}$$

$$\frac{d(\tilde{\mu}_2 u)}{dz} = K_{tc}(\lambda_2\tilde{\lambda}_0 + 2\lambda_1\tilde{\lambda}_1 + \lambda_0\tilde{\lambda}_2) - K_{d2}\tilde{\mu}_2 + (K_{tfm}[M] + K_\beta)\tilde{\lambda}_2 + K_{fp}\left((\lambda_2 + \tilde{\lambda}_2)\tilde{\mu}_1 - \lambda_{to}\tilde{\mu}_3\right) \tag{27}$$

Temporary polymer $\tilde{\tilde{P}}$

$$\frac{d\left(\tilde{\tilde{\mu}}_0 u\right)}{dz} = K_{tc}\tilde{\lambda}_0^2 - 2K_{d2}\tilde{\tilde{\mu}}_0 \tag{28}$$

$$\frac{d\left(\tilde{\tilde{\mu}}_1 u\right)}{dz} = K_{tc}\tilde{\lambda}_o\tilde{\lambda}_1 - 2K_{d2}\tilde{\tilde{\mu}}_1 \tag{29}$$

$$\frac{d\left(\tilde{\tilde{\mu}}_2 u\right)}{dz} = K_{tc}\left(\tilde{\lambda}_0\tilde{\lambda}_2 + \tilde{\lambda}_1^2\right) - 2K_{d2}\tilde{\tilde{\mu}}_2 \tag{30}$$

Obviously, an update of the second moments requires a third moment term (μ_3), which thus makes the system equations open ended. Hulburt and Katz[18] solved the problem of moment closure by approximating higher moments using Laguerre functions about Γ distributions and got the following expressions:

$$\mu_3 = \frac{\mu_2}{\mu_0\mu_1}(2\mu_0\mu_2 - \mu_1^2) \tag{31}$$

$$\tilde{\mu}_3 = \frac{\tilde{\mu}_2}{\tilde{\mu}_0\tilde{\mu}_1}(2\tilde{\mu}_0\tilde{\mu}_2 - \tilde{\mu}_1^2) \tag{32}$$

LDPE polymer chains are branched. Studies have shown that polymers produced in vessel reactors are more branched than those produced in tubular reactors.[19] However, the detection of branching is not easily achievable in as much as it is important to industrial applications because the presence of branches impacts polymer processing. Chain transfer controls the chain length and causes branching. An internal radical center is a radical located on a backbone carbon atom and is generated through two reactions: transfer to polymer and back-biting. These internal radical centers can undergo all reactions that chain-end radicals undergo and then propagate,

which leads to branching. Long-chain branches (LCBs) and short-chain branches (SCBs) are formed through the reactions of transfer to polymer and back-biting, respectively:

$$\frac{d(uC_{\mathrm{LCB}})}{dz} = K_{\mathrm{LCB}}\lambda_{to}(\mu_1 + \tilde{\mu}_1) \tag{33}$$

where C_{LCB} is the long-chain branching concentration and

$$K_{\mathrm{LCB}} = \frac{K_p K_{fp}\,[\mathrm{M}]}{K_p[\mathrm{M}] + K_\beta + K_{tfm}[M]} \tag{34}$$

K_{LCB} is the long-chain branching rate constant, L/mol.s. In a back-biting reaction, the radical activity of the polymer chain is transferred to a site along the same chain, thus generating a SCB, whose concentration variation is expressed by

$$\frac{d(uC_{\mathrm{SCB}})}{dz} = K_{\mathrm{SCB}}\lambda_{to} \tag{35}$$

where C_{SCB} is the short-chain branching concentration and

$$K_{\mathrm{SCB}} = \frac{K_p K_b[\mathrm{M}]}{K_p[\mathrm{M}] + K_\beta + K_{tfm}[\mathrm{M}]} \tag{36}$$

K_{SCB} Long-chain branching rate constant, L/mol. sAlternatively, β scission of secondary and tertiary radicals can also produce vinyl and vinyledene groups. The integration of the model, along with an update of the transport and thermodynamic properties, gives the concentrations of all reacting species in terms of the reactor length. The monomer conversion (y_m) and the weight and number averages of molecular weight averages [$M_w(z)$ and $M_n(z)$, respectively] are expressed, respectively, as

$$y_m(z) = 1 - \frac{[\mathrm{M}(z)]u(z)}{[\mathrm{M}]_0 u_0} \tag{37}$$

$$M_w(z) = \frac{M_{wm}\left\{\mu_2(z) + \tilde{\mu}_2(z) + \tilde{\tilde{\mu}}_2(z) + \lambda_2(z) + \tilde{\lambda}_2(z)\right\}}{\mu_1(z) + \tilde{\mu}_1(z) + \tilde{\tilde{\mu}}_1(z) + \lambda_1(z) + \tilde{\lambda}_1(z)} \tag{38}$$

$$M_n(z) = \frac{M_{wm}\left\{\mu_1(z) + \tilde{\mu}_1(z) + \tilde{\tilde{\mu}}_1(z) + \lambda_1(z) + \tilde{\lambda}_1(z)\right\}}{\mu_0(z) + \tilde{\mu}_0(z) + \tilde{\tilde{\mu}}_0(z) + \lambda_0(z) + \tilde{\lambda}_0(z)} \tag{39}$$

where $[\mathrm{M}]_0$ is the monomer concentration at the reactor inlet and M_{wm} is the monomer molecular weight. The distribution of the sizes of polymer chains is not completely defined by its central tendency. Thus, it is desirable to determine the breadth and shape of the distribution curve, and this is appropriately done with the aid of parameters defined from the moments of distribution. The ratio of the weight-average molecular weight (M_w) to the number-average molecular weight (M_n) is defined to estimate the polydispersity of a sample. With the moments of each polymer, a Wesslau distribution is used to construct the instantaneous molecular weight distribution (MWD) of a polymer:[20]

$$W(\ln M_{ww}) = \frac{\exp\left(-[\ln(M_{ww}) - \mathrm{Ln}(\bar{\varphi})]^2/(2\sigma^2)\right)}{\sigma\sqrt{2\pi}} \tag{40}$$

where M_{ww} is the molecular weight of a polymer chain of length r.

$$\sigma^2 = \ln\left(\frac{M_w}{M_n}\right) \tag{41}$$

$$\bar{\varphi} = M_n \exp\left(\frac{\sigma^2}{2}\right) \tag{42}$$

W is the Wesslau distribution, σ is the variance of the polymer chain population defined by equation (41), $\bar{\varphi}$ is the average weight of the molecular weights of the polymer chains. The reactor model and the polymer kinetic model were integrated together with a variable-order solver on the basis of the numerical differentiation formulas for stiff differential equations in a Matlab environment. The reliable integration of the model requires good information on the transport and thermodynamic properties, which are listed in Table AI (see Appendix). Thus, the transport and thermodynamic properties of the reaction mixture are updated along the reactor length to ensure the adequacy of the model predictions.

Injection and mixing point equations

The computation of the mixture conditions is quite delicate after the injection of a fresh side stream. When the operation of a tubular reactor is simulated with lateral feed streams, the mass, momentum, and energy balances should be solved simultaneously to determine the velocity and temperature of the reaction mixture as well as the concentrations of components after the injection point. Lateral feed streams are assumed to be at the same pressure as the main reaction mixture at the point of injection. $\overline{M}$ and $\overline{I}$ are the molar flow rates of the monomer and the initiator in the lateral stream, and the process variables entering the mixing point are indicated by a subscript *e*. The flow condition of the process stream exiting the mixing point is determined by the simultaneous solution of the mass flow and energy balance equations, which are shown next.

Mass flow balance

$$u_f \rho_f = u_e \rho_e + \frac{28\bar{M} + M_{wi}\bar{I}}{A_s} \tag{43}$$

where the subscript f indicates the condition after the mixing point and M_{wi} is the molecular weight of the initiator.

Molar flow balances for each component

$$u_f[\mathrm{M}]_f = u_e[\mathrm{M}]_e + \frac{\bar{M}}{A_s} \tag{44}$$

$$u_f[\mathrm{I}]_f = u_e[\mathrm{I}]_e + \frac{\bar{I}}{A_s} \tag{45}$$

where A_s is the pipe cross-section area. Similarly

$$u_f[\mathrm{X}]_f = u_e[\mathrm{X}]_e \tag{46}$$

where [X] stands for any molar concentration: μ_i, $\tilde{\mu}_i$, $\tilde{\tilde{\mu}}_i$, C_{LCB}, or C_{SCB}.

Energy balance

The local temperature results from an enthalpy balance between the main flow and the lateral feed streams, and it is expressed as

$$C_{pf}T_f = \frac{A_s \rho_e u_e C_{pe} T_e + \left(28\bar{M} + M_{wi}\bar{I}\right)\bar{C}_p\bar{T}}{A_s \rho_f u_f} \tag{47}$$

$\bar{T}$ is the temperature of the lateral stream, K.
Where $\bar{C}_p$ is set equal to the ethylene heat capacity and C_{pf} is the reaction mixture heat capacity given by

$$C_{pf} = 0.518 w_m + (1.041 + 8.3\times10^{-4}\ T) w_p \tag{48}$$

where w_m and w_p are the weight fractions of the monomer and polymer, respectively, after the mixing point and are expressed as

$$w_m = \frac{\dot{m}_f\, u_f A_s}{\dot{\bar{m}} + \left(\dot{m} + \dot{m}_p\right)_e u_e A_s} \quad \text{and} \quad w_p = 1 - w_m \tag{49}$$

$\bar{m}$ is the monomer mass flow rate in the lateral stream, kg/s.
Where $\dot{m}$ is the monomer mass flow rate (kg/s). Because only a small amount of initiator is added, its contribution to the density and heat capacity is neglected. The nonlinear eqs. (43), (44), and (47) were solved simultaneously for M_f, u_f, and T_f by the Gauss–Newton method. In the reactor section following the injection point, the monomer conversion is defined as

$$y_m(z) = \left(1 - \frac{[\mathrm{M}(z)]u(z)A_s}{[\mathrm{M}]_o u_o A_s + \bar{M}}\right) \tag{50}$$

where the subscript o refers to the initial condition at the reactor inlet. At the next injection point, the conversion is updated again.

RESULTS AND DISCUSSION

Continuous stirred tank reactor (CSTR) kinetic model validation

The performance of the two difunctional initiators 2,2-bis(*tert*-butylperoxy) butane (BU) and 2,5-dimethylhexane-2-*tert*-butylperoxy-5-perpivalate (DHBPPI) was compared with that of dioctanoyl (DCT) for ethylene polymerization in a high-pressure tubular reactor. First, the experimental data obtained by Luft and coworkers[13,14] were collected and served to validate the kinetic model previously developed for ethylene polymerization initiated with difunctional initiators in an autoclave reactor.[15] For comparison, the ethylene conversion obtained with each initiator is plotted in Figure 2.

Because of the dissimilar decomposition rate of the peroxides, each initiator was effective only over a given temperature range, depending on its half-life temperature. With respect to dioctanoyl peroxide, the BU initiator required only half the amount of DCT to nearly double the conversion with less reaction time but at the expense of a higher thermal energy. In a similar comparison, the second difunc-

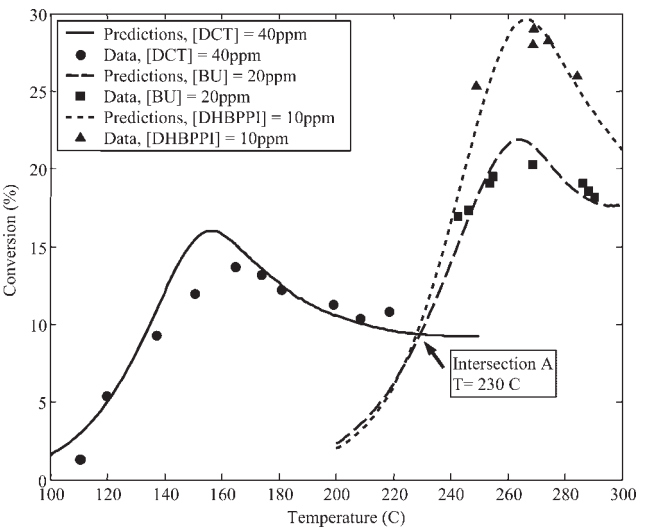

Figure 2 Prediction and data conversion of ethylene versus temperature: DCT $[\mathrm{I}]_o$ = 40 ppm and θ_r = 65 s, BU $[\mathrm{I}]_o$ = 20 ppm and θ_r = 40 s, DHBPPI $[\mathrm{I}]_o$ = 10 ppm and θ_r = 60 s, and P = 1700 bar. θ_r is the autoclare reaction resisdence time, S.

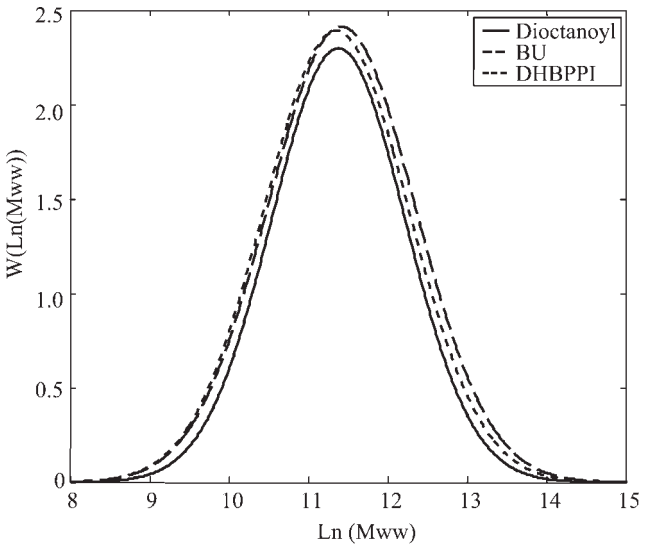

Figure 3 Prediction of the MWD of PE for the different initiators, DCT, BU, and DHBPPI. P = 1700 bar, T = 230°C, $[I]_o$ = 20 ppm, and θ_r = 60 s.

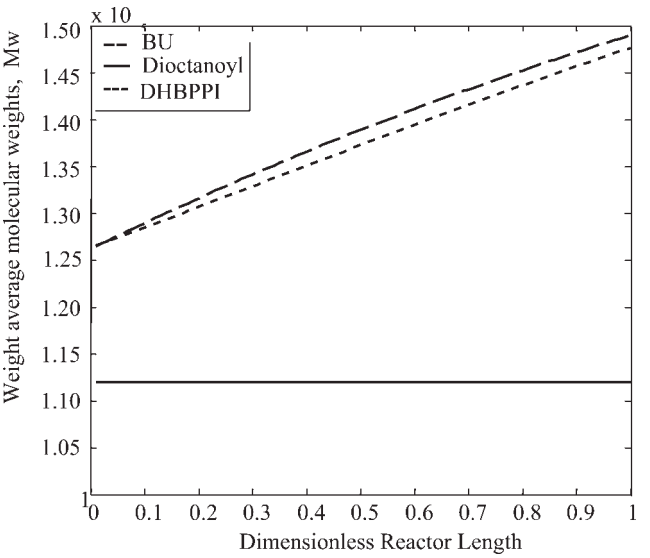

Figure 4 Comparison of the $M_w(z)$ values along the tubular reactor for the different initiators at a constant temperature of 230°C.

tional initiator (DHBPPI) performed even better. Thus, dioctanoyl peroxide was better suited for temperatures around 165°C, whereas the difunctional counterparts started reacting only when the temperature exceeded 200°C. At intersection point A (230°C), all three peroxides produced approximately the same conversion. A plot of the MWD is given in Figure 3, and it shows that difunctional peroxides produced polymers with broader MWDs than DCT. The breadth of polymer chain distribution affects the end-product properties and the energy requirements in polymer processing. In principle, running ethylene polymerization in a tubular reactor does not affect the kinetic rate constants, but it affects the monomer conversion and polymer characteristics such as branching.

LDPE tubular reactor

In an industrial setting, the reactor temperature is prevented from exceeding its ceiling limit by manipulation of the feed temperature and pressure as well as the initiator flow rate. Zimmermann and Pollok[21] discussed the influence of the initiator type on the peak reaction temperature. Alternatively, a better way of monitoring the reaction behavior inside the tubes is to keep the jacket temperature constant in each zone.[22] Nevertheless, the reactor operation is predominantly nonisothermal unless an efficient optimal control scheme is implemented. For instance, running the reactor at a constant temperature of 230°C helps to determine how the polymer molecular weight varies according to the initiator type. In fact, M_w plots in Figure 4 show that a high molecular weight was obtained with peroxides BU and DHBPPI compared to DCT at the same temperature.

The production of polymers with high molecular weights is another good reason to use difunctional organic peroxides as initiators. Therefore, the preceding analysis done on the performance of the three initiators can be used as a guideline to select the appropriate initiator that corresponds to a specific zone of reaction. Obviously, each of the three initiators has to be used within a given operating temperature range to maximize its contribution to the polymerization of ethylene. For a better assessment of the peroxides' performance in the polymerization of ethylene, a sequential quadratic programming (SQP) optimization procedure was accomplished to determine the optimal wall temperature in each zone. The SQP maximization of ethylene conversion generated the optimal operating conditions tabulated in Table III.

The optimal initial concentrations of the peroxides DCT, BU, and DHBPPI were 27.3, 14.8, and 10.4 ppm, respectively. Subsequently, the process behavior was analyzed at the optimal conditions. For instance, Figure 5 shows profiles of the optimal reactor temperature and jacket temperature for each initiator along the reactor. Intrinsically, the correspond-

TABLE III
Optimal Operating Conditions for the LDPE Tubular Reactor

Initiator	$T_{c,zone1}$ (°C)	$T_{c,zone2}$ (°C)	$T_{c,zone3}$ (°C)	[I] (ppm)
DCT	107.6	150.12	101.7	27.3
BU	223.35	211.65	193.16	14.8
DHBPPI	232.9	209.45	185.4	10.4

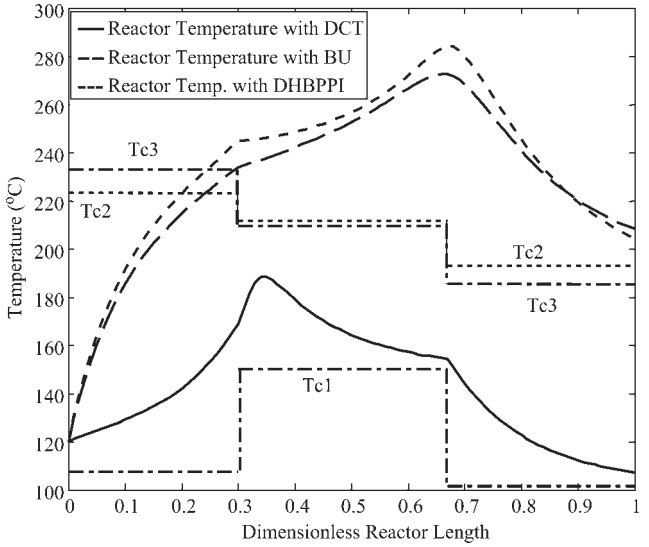

Figure 5 Profiles of the optimal reactor and optimal jacket temperatures (T_{c1}, T_{c2}, and T_{c3}) for the DCT, BU, and DHBPPI initiators, respectively. T_{cj} (j = 1,2,3) is the Cooling jacket temperature for initiator j as in Figure 5, K.

ing evolution of ethylene conversion is shown in Figure 6. As the reaction temperature approached 190°C (peak temperature), the effectiveness of the DCT peroxide slowed down, and therefore, ethylene conversion reached a plateau.

Alternatively, the reactivity of the peroxides BU and DHBPPI exhibited better performances at higher temperatures, ranging from 260 to 300°C. Maximum ethylene conversions of 13.35, 19.4, and 22.9% were reached with the optimal initial concentrations of 27.3, 14.8, and 10.4 ppm for DCT, BU, and DHBPPI, respectively. Therefore, the DHBPPI peroxide yielded the highest conversion with the lowest initial

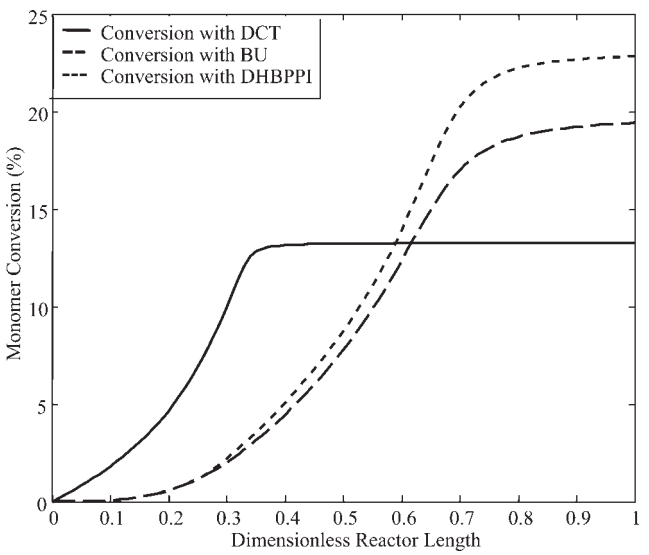

Figure 6 Ethylene conversion profiles for the different initiators.

initiator amount. Upon observing the temperature and conversion evolution along the reactor, we concluded that the high-temperature profiles computed for the peroxides BU and DHBPPI in the first half of the reactor length did not necessarily boost ethylene conversion, and therefore, the DCT peroxide remained the preferred initiator over the first half of the reactor with an operating temperature lower than 190°C. Furthermore, optimal wall temperatures were determined such that each initiator was compelled to perform at its best. This was accomplished by a gradual increase of the reactor temperature so that the initiator was not brought too soon to thermal conditions that sped up its depletion. Therefore, these observations demonstrate clearly that the use of the second group of peroxides resulted in a higher LDPE productivity, which was expressed in terms of higher ethylene conversions and lower amounts of initiators.

Under isothermal conditions (Fig. 4), the model predicts high average molecular weight profiles with the peroxides BU and DHBPPI compared to polymer obtained with the monofunctional peroxide. However, under nonisothermal operations, the thermal energy required to obtain a high conversion precipitates the polymer chains to end sooner and, hence, produce polymers with low M_n and M_w values (Fig. 7).

Alternatively, in accordance with the DCT kinetic reactivity, operating the reactor at a low temperature level results in higher polymer average molecular weights but at the expense of low conversion.

LDPE polymers formed in high-pressure reactors are branched chains and exhibit remarkable rheological properties. Yamaguchi and Takahashi[19] studied the effect of branching on LDPE and found that autoclave reactors produce polymers with higher numbers of branching than the polymers formed in tubular reactors. A broad MWD, a high polydispersity index, and the presence of branching can certainly impact the polymer properties. Chain transfer to polymer and terminal double-bond polymerization are commonly known factors that cause branches to grow on a polymer. The plots in Figure 8 show that the presence of significant long-chain branches (LCBs) and SCBs is related to difunctional peroxides. In particular, the introduction of LCBs is advantageous for polymer processing, as it improves the melt strength.[10,19]

Figure 1 shows the injection of lateral reactant feeds to the tubular reactor. Side streams 2 and 3 were placed at 30 and 67% of the total length, respectively. Next, three simulation scenarios of injecting the reactant streams were considered with the difunctional initiator BU only. In the first scenario, no splitting of the feed streams was considered; it was identical to the simulation runs done so

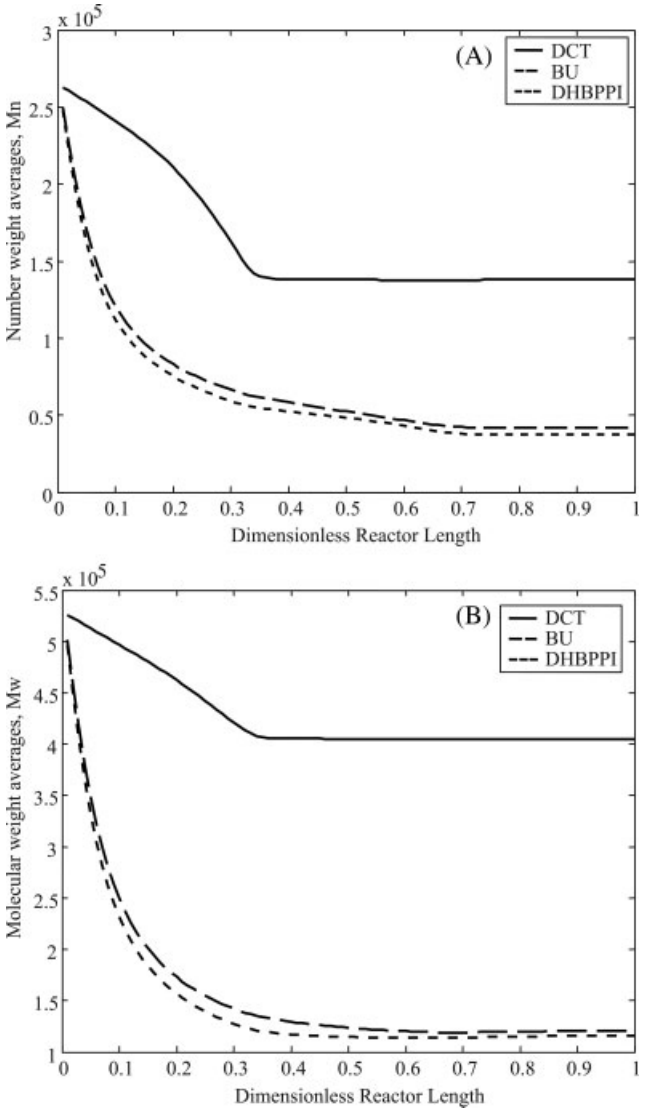

Figure 7 Comparison of (A) M_n and (B) M_w values along the tubular reactor for DCT, BU, and DHBPPI.

far. In the second run, only the initiator was split on the basis of 50 mol % at the reactor inlet and 25 mol % at each injection point, and ethylene was entirely fed into stream 1. In the third run, half of each of the monomer and initiator amounts was fed into the reactor entrance, and the remaining 50% of the mixture was equally split and constituted the two lateral streams.

Variations of the process variables are shown in Figure 9(A–F) for all three simulation runs. The temperature profiles in Figure 9(A) exhibit one, two, and three peaks for runs 1, 2 and 3, respectively. These thermal variations were specific to the way the reactor was operated and the way the lateral streams were distributed. Temperature and monomer conversion were highly interdependent process variables (plots A and B). With no side injection, ethylene conversion (solid line) rose gradually and reached a final value around 15%. In run 2, ethylene conversion (dotted line) was relatively slow at first because the initial initiator amount was halved; then, it took off as more initiator was added at injection location 2, and then, at location 3, it reached a higher final value around 21.5%. In run 3, only half of the reacting mixture was fed into the reactor inlet, and the other half was equally distributed between the two lateral injections. In fact, keeping the heating–cooling utility conditions invariant and halving the monomer amount allowed the reactor temperature to rise quickly in the first quarter of the reactor, as shown in plot A (run 3). Then, the addition of an intermediate cold monomer stream lowered the reaction thermal content, as a result of which, the mixture temperature dropped suddenly.

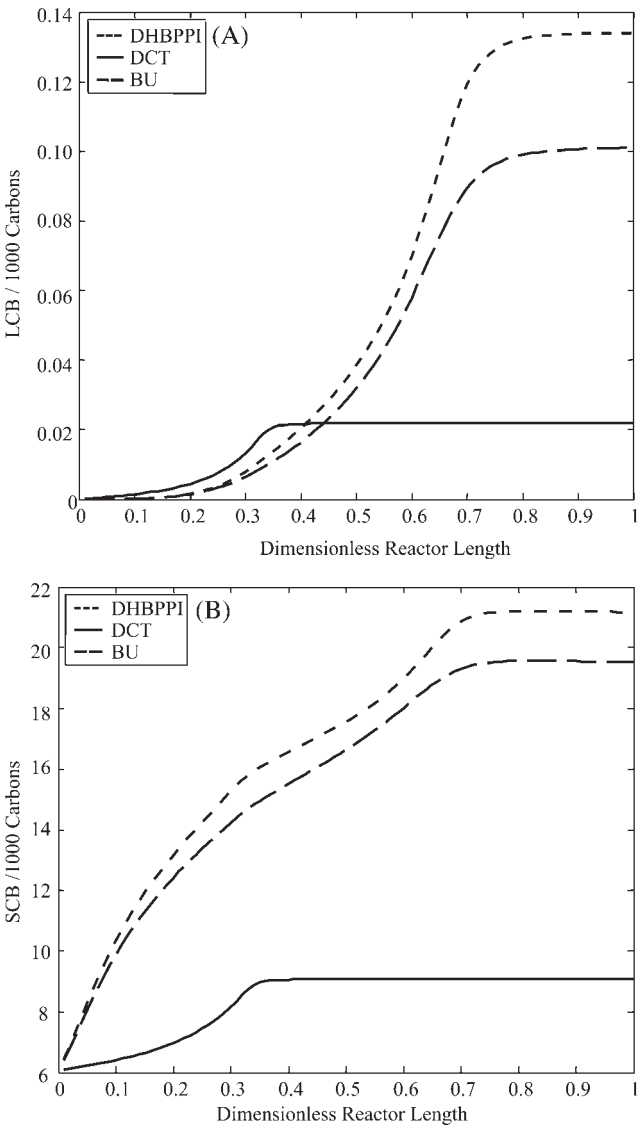

Figure 8 Prediction of (A) LCB and (B) SCB frequency for the different initiators.

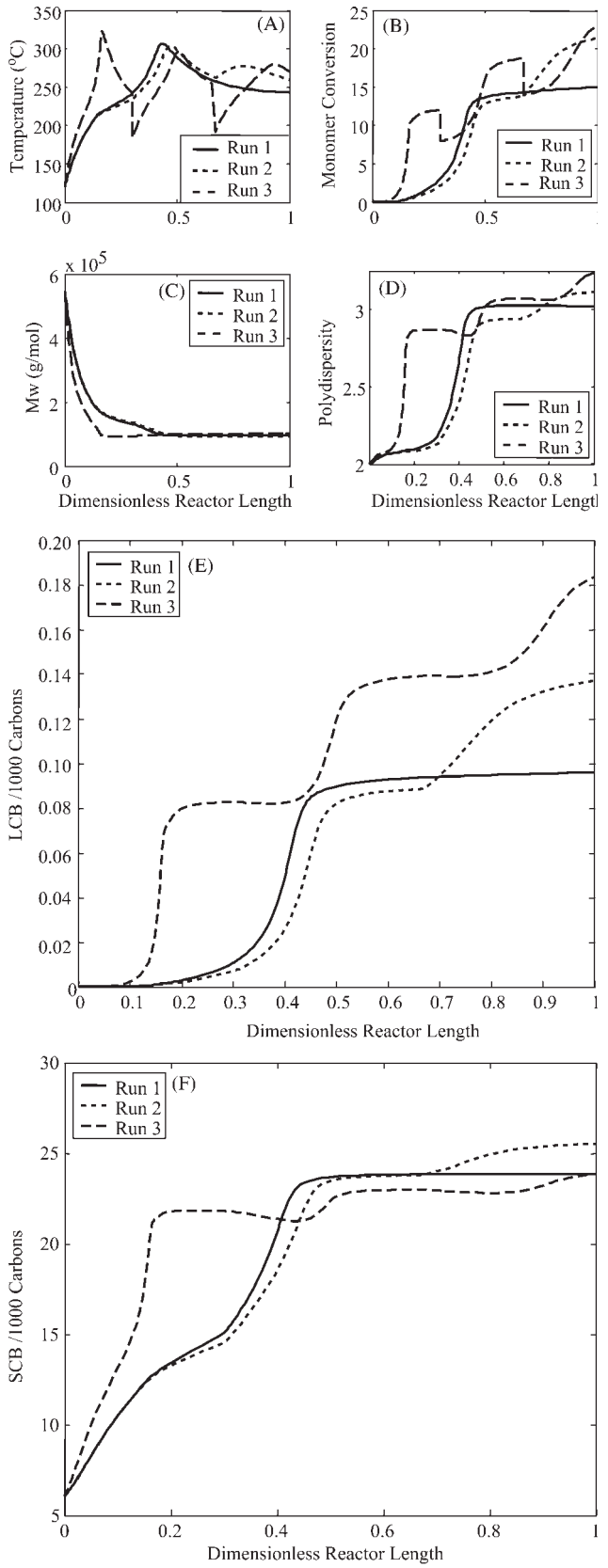

Figure 9 Effect of the injection ethylene and BU initiator in lateral streams: (run 1) main stream only, (run 2) injection of 50% initiator in two lateral streams, and (run 3) injection of 50% initiator and monomer equally split into two lateral streams.

Once the incoming side stream was completely blended with the hot bulk flow, the reactor temperature and ethylene conversion started increasing gradually until the next the injection point. However, it is important to emphasize that the sudden sharp drop in conversion recorded at the injection point in run 3 did not mean a degeneration of the reaction, but it was mainly due to the fact that the conversion new update took into account the freshly injected monomer amount. Correspondingly, whereas the first rapid temperature rise (dashed line) caused a steep ascent of ethylene conversion, it significantly lowered the average polymer molecular weight. Furthermore, the lateral injection of the initiator alone (run 2) did not much affect the average molecular weight, but it produced more branches in the polymer. On the other hand, the monomer side stream increased the polydispersity index and produced more branched polymer, but at the first injection, it generated a sharp rise in SCBs, which settled quickly to a plateau close to the levels obtained in the other simulation runs.

CONCLUSIONS

In this article, we proposed a new kinetic model for LDPE production using difunctional initiators in high-pressure tubular reactor. We accounted for the thermodynamic and transport properties of the high-pressure process. Kinetic rate constants were determined from CSTR experimental data collected from the literature. For the nonisothermal tubular reactor, an SQP optimization scheme was used to determine a suitable wall temperature for each zone. In comparison with dioctanoyl peroxide, lesser amounts of BU and DHBPPI peroxide were required to get higher conversions in shorter reaction times but at the expense of high thermal energies. The difunctional peroxides became effective only for reactor temperatures above 240°C. They produced polymers with higher molecular weights and are recommended for use in the second half of the reactor. The results also show that polymers produced with the difunctional peroxides had broader MWDs and contained more branching. Injecting fresh ethylene at different points along the reactor improved the conversion and produced more branched polymers.

NOMENCLATURE

A	frequency factor (s^{-1} or L/mol s)
A_p	pipe surface area (cm^2)
A_s	pipe cross-section area (cm^2)
C_j	molar concentration (mol/cm^3)
C_{LCB}	long-chain branching concentration (mol/L)

C_p, $\overline{C}_p$	heat capacity (cal g^{-1} K^{-1})
C_{pf}	reaction mixture heat capacity
C_{SCB}	short-chain branching concentration (mol/L)
D_i	inside diameter of the reactor (cm)
D_o	outer diameter of the reactor (cm)
E	activation energy (cal/mol)
E_v	activation energy for viscous flow (kJ/Kmol)
f_1	efficiency of the original initiator
f_2	efficiency of the initiator with undecomposed peroxide
F_j (j = M or I)	molar flow rate of the monomer and initiators (mol/s)
f_r	fanning friction factor (dimensionless)
h_i	inside film heat-transfer coefficient (cal cm^{-2} s^{-1} K^{-1})
h_w	wall (reactor) heat-transfer coefficient (cal cm^{-2} s^{-1} K^{-1})
I	initiator molecule
[I]	initiator concentration (mol/L)
$\overline{I}$	initiator molar flow rate (mol/s)
k	thermal conductivity of the reaction mixture (cal cm^{-1} s^{-1} K^{-1})
K_1, K_2	rate constants for initiation (s^{-1})
K_b	rate constant for back-biting (s^{-1})
K_{d1}	decomposition rate constant of the original difunctional peroxide (s^{-1})
K_{d2}	decomposition rate constant of the peroxide with an undecomposed radical (s^{-1})
K_{fp}	rate constant for transfer to polymer (L mol^{-1} s^{-1})
K_p	rate constant for propagation (L mol^{-1} s^{-1})
K_{tc}	rate constant for termination (L mol^{-1} s^{-1})
K_{tfm}	rate constant for transfer to mono mer (L mol^{-1} s^{-1})
K_{th}	rate constant for thermal initiation (L^2 mol^{-2} s^{-1})
L	reactor length (m)
M	monomer molecule
[M]	monomer concentration (mol/L)
$\overline{M}$	monomer molar flow rate (mol/s)
$\dot{m}$	monomer mass flow rate (kg/s)
$[M]_0$	monomer concentration at the reactor inlet
$\dot{m}_c$	cooling mass flow rate (kg/s)
M_n	number-average molecular weight (g/mol)
$M_n(z)$	number-average molecular weight average (g/mol)
M_w	weight-average molecular weight (g/mol)
M_{wi}	molecular weight of the initiator
M_{wm}	monomer molecular weight (g/mol)
M_{ww}	molecular weight of a polymer chain of length r
$M_w(z)$	weight-average molecular weight average (g/mol)
Nu	Nusselt number
P	polymer molecule
P	pressure (bar)
$\tilde{P}$	dead polymer molecule with one decomposed peroxide
$\tilde{\tilde{P}}$	dead polymer molecule with two undecomposed peroxides
P_c	critical pressure (MPa)
Pr	Prandtl number (dimensionless)
P_r	dead polymer molecule
P_r	dead polymer concentration (mol/L)
$\tilde{P}_r$	dead polymer concentration with one undecomposed peroxide (mol/L)
$\tilde{\tilde{P}}_r$	dead polymer concentration with two undecomposed peroxides (mol/L)
q	total flow rate of reactants in a CSTR (L/s)
R_1, R_2	organic group of the peroxide
Re	Reynolds number (dimensionless)
R_I	rate of initiation without undecomposed peroxide
$\tilde{R}_I$	rate of initiation with undecomposed peroxide
$R^{\bullet}_{in}$	primary initiator radical fragment
$\tilde{R}^{\bullet}_{in}$	initiator radical fragment with one undecomposed peroxide
R_p	rate of polymerization (mol s^{-1} L^{-1})
$R^{\bullet}_r$	radical of chain length r
$\tilde{R}^{\bullet}_r$	macroradical fragment of chain length r with one undecomposed peroxide
$R^{\bullet}_s$	radical of chain length s
$\tilde{R}^{\bullet}_s$	macroradical fragment of chain length s with one undecomposed peroxide
T	reaction temperature (K)
T_c	cooling process temperature (K) or critical temperature (K)
T_r	reduced temperature
u	reaction mixture velocity (cm/s)
U	overall heat-transfer coefficient (cal cm^{-2} s^{-1} K^{-1})
$V_{M,E}$	specific volume of the reaction mixture (cm^3/g)
$V_{P,E}$	specific volume of the polymer (cm^3/g)
w	weight fraction

[X] any molar concentration: μ_i, $\tilde{\mu}_i$, $\tilde{\tilde{\mu}}_i$, C_{LCB}, or C_{SCB}
y_m monomer conversion
z reactor length (cm)

Subscripts

β β scission
e process condition before the injection point
f condition after the mixing point
I initiator
m monomer
p polymer
r chain length
o initial condition at the reactor inlet

Greek letters

Δv activation volume (cm^3/mol)
$-\Delta H_R$ heat of reaction (cal/mol)
η dense gas viscosity of the monomer (Pa s)
η^0 low-pressure monomer viscosity (Pa s)
η^s viscosity of the gas mixture, Pa.s
λ_i moment of the live temporary polymer radical (i = 0, 1, 2)
$\tilde{\lambda}_i$ moment of the live temporary polymer radical with one undecomposed peroxide (i = 0, 1, 2)
λ_{to} total concentration of radicals (mol/L)
μ_i moment of the polymer molecule (i = 0, 1, 2, 3)
$\tilde{\mu}_i$ moments of the temporary polymer molecule (i = 0, 1, 2, 3)
$\tilde{\tilde{\mu}}_i$ moment of the dead polymer molecule with two undecomposed peroxides (i = 0, 1, 2)
ρ density (g/cm^3)
ρ_r reduced density
ξ defined in Table AI $(Pa\ s)^{-1}$
ξ expression in the intrinsic viscosity η^0 (Table AI)

APPENDIX

Moments of polymer species

Polymer species consist of growing radical chains, dead polymer chains, and two different polymer chains with one and two undecomposed peroxides.

TABLE AI
Transport and Thermodynamic Properties

	Reference
Property expression	
$\rho = [1 + 0.028[M](V_{P,E} - V_{M,E})]/V_{P,E}$	
$V_{M,E} = (3.7994 - 0.2610978\ \text{Ln}\ P - 0.6944404\ \text{Ln}\ T + 0.0632416\ \text{Ln}\ T \times \text{Ln}\ P)^{-1}$	Feucht et al.[23]
$V_{P,E} = 9.61 \times 10^{-7} + 7.0 \times 10^{-10}\ T - 5.3 \times 10^{-11}\ P$	Feucht et al.[23]
$C_p = 0.518(1 - y_m) + (1.041 + 8.3 \times 10^{-4}\ T)y_m$	Kalyon et al.[24]
$\Delta H_R = [84.185 \times 10^3 + 0.209(T - 273) + 0.105P)/4.1868$	Kiparissides et al.[6]
Heat-transfer coefficient	
$U^{-1} = h_i^{-1} + h_w^{-1}$	
$h_i = kNu/D_i$	
$h_w = 0.03$	
$k = 5 \times 10^{-4}(1 - y_m) + 3.5 \times 10^{-4}\ y_m$	
$Nu = 0.166(Re^{2/3} - 125)Pr^{0.33}[1 + (D_i/L)^{2/3}]$, for $Re < 10{,}000$	
$Nu = 0.026Re^{0.8}Pr^{0.33}$, for $Re > 10{,}000$	
$Pr = C_p\eta_S/k$, $Re = \rho u D_i/\eta_S$	
$\eta_S = \eta\ \exp[2 + 0.001a_v(\mu_1/\mu_0)^{0.556} \times \mu_1 + E_v/R(1/T - 1/423)]$	
$[(\eta - \eta^0)\xi + 1]^{0.25} = 1.023 + 0.2336\rho_r + 0.58533\rho_r^2 - 0.40758\rho_r^3 + 0.09332\rho_r^4$	Reid et al.[25]
$\xi = 10^7\{T_c/[M' \times (9.869P_c)^4\}^{1/6}$	Reid et al.[25]
$\eta^0\xi = 4.61T_r^{0.618} - 2.04\ \exp(-0.449T_r) + 1.94\ \exp(-4.058T_r) + 0.1$	Poling et al.[26]
$E_v = -4.1868(500 - 560\mu_1)$	
μ_1 = viscosity	

$V_{P,E}$ = specific volume of the polymer; $V_{M,E}$ = specific volume of the reaction mixture; h_i = inside film heat-transfer coefficient; h_w = wall (reactor) heat-transfer coefficient; Nu = Nusselt number; k = thermal conductivity of the reaction mixture; Pr = Prandtl number; E_v = activation energy for viscous flow; η = dense gas viscosity of the monomer; η^0 = low-pressure monomer viscosity; ρ_r = reduced density; P_c = critical pressure; T_r = reduced temperature; T_c = critical temperature; a_v=0.018; M′=ethylene molecular weight (g/mol).

Concentration of the temporary polymer radicals

$$\lambda_i = \sum_{r=1}^{\infty} r^i [R_r^\bullet] \quad (A.1)$$

$$\tilde{\lambda}_i = \sum_{r=1}^{\infty} r^i [\tilde{R}_r^\bullet] \quad (A.2)$$

where the superscript i is 0, 1, and 2 for the zeroth, first, and second moments, respectively. The total concentration of radical species includes radicals with an undecomposed peroxide group and radicals without any undecomposed peroxide group:

$$\lambda_{to} = \lambda_0 + \tilde{\lambda}_0 \equiv \sum_{r=1}^{\infty} [R_r^\bullet] + \sum_{r=1}^{\infty} [\tilde{R}_r^\bullet] \quad (A.3)$$

Moments of dead polymers

$$\mu_i = \sum_{r=1}^{\infty} r^i [P_r] \quad (A.4)$$

Moments of dead polymers related to the undecomposed peroxide [i.e., $\tilde{P}_r$:(R—$\tilde{R}$) and $\tilde{\tilde{P}}_r$:($\tilde{R}$—$\tilde{R}$) (see Table AI)]

$$\tilde{\mu}_i = \sum_{r=1}^{r} i [\tilde{P}_r] \quad (A.5)$$

$$\tilde{\tilde{\mu}}_i = \sum_{r=1}^{\infty} r^i [\tilde{\tilde{P}}_r] \quad (A.6)$$

References

1. Goto, S.; Yamamoto, K.; Furui, S.; Sugimoto, M. J Appl Polym Sci 1981, 36, 21.
2. Chan, W. M.; Gloor, P. E.; Hamielec, A. E. AIChE J 1993, 39, 111.
3. Brandolin, A.; Lacunza, M. H.; Ugrin, P. E.; Capiati, N. J Polym React Eng 1996, 4, 193.
4. Baltsas, A.; Papadopoulos, E.; Kiparissides, C. Comp Chem Eng 1998, 22 (Suppl.), S95.
5. Marini, L.; Georgakis, C. AIChE J 1984, 30, 409.
6. Kiparissides, C.; Verros, G.; MacGregor, J. F. J Macromol Sci Rev Macromol Chem Phys 1993, 33, 437.
7. Seidl, H.; Luft, G. J Macromol Sci Chem 1981, 15, 1.
8. Suyama, S.; Ighigaki, H.; Nakamura, T.; Sugihara, Y.; Kamura, H.; Watanabe, Y. Polym J 1994, 26, 273.
9. Scorah, M. J.; Dhib, R.; Penlidis, A. J Polym Sci Part A: Polym Chem 2004, 42, 5647.
10. Scorah, M. J.; Tzoganakis, C.; Dhib, R.; Penlidis, A. J Appl Polym Sci 2007, 103, 1340.
11. Perez, C. J.; Cassano, G. A.; Valles, E. M.; Failla, M. D.; Quinzani, L. M. Polymer 2002, 43, 2711.
12. Kondratiev, J. N.; Ivantchev, S. S. Chem Eng J 2001, 107, 221.
13. Luft, G.; Seidl, H. Angew Makromol Chem 1985, 129, 61.
14. Luft, G.; Dorn, M. J Macromol Sci Chem 1988, 25, 987.
15. Dhib, R.; Al-Nidawy, N. Chem Eng Sci 2002, 57, 2735.
16. Villalobos, M. A.; Hamielec, A. E.; Wood, P. E. J Appl Polym Sci 1991, 42, 629.
17. Zabinsky, R. C. M.; Chan, W. M.; Gloor, P. E.; Hamielec, A. E. Polymer 1992, 33, 2243.
18. Hulburt, H. M.; Katz, S. Chem Eng Sci 1964, 19, 555.
19. Yamaguchi, M.; Takahashi, M. Polymer 2001, 42, 8663.
20. Friis, N.; Hamielec, A. E. J Appl Polym Sci 1975, 19, 97.
21. Zimmermann, H.; Pollok, T. Plastics, Rubber and Composites Processing and Applications 1998, 27, 12.
22. Asteasuain, M.; Tonelli, S. M.; Brandolin, A.; Bandoni, J. A. Comput Chem Eng 2001, 25, 509.
23. Feucht, P.; Tilger, B.; Luft, G. Chem Eng Sci 1985, 40, 1935.
24. Kalyon, D. M.; Chiou, Y. N.; Kovenklioglu, S.; Bouaffar, A. Polym Eng Sci 1994, 33, 804.
25. Reid, R. C.; Prausnitz, J. M.; Sherwood, T. K. The Properties of Gases and Liquids; McGraw-Hill: New York, 1977.
26. Poling, B. E.; Prausnitz, J. M.; O'Connel, J. P. The Properties of Gases and Liquids, 5th ed.; McGraw-Hill: New York, 2001.